

## Linking ozone pollution and climate change: The case for controlling methane

Arlene M. Fiore, Daniel J. Jacob, and Brendan D. Field

Department of Earth and Planetary Sciences and Division of Engineering and Applied Sciences,  
Harvard University, Cambridge, MA, USA

David G. Streets and Suneeta D. Fernandes

Argonne National Laboratory, Argonne, IL, USA

Carey Jang

USEPA/OAQPS MC: D243-01, RTP, NC, USA

Received 4 June 2002; revised 8 August 2002; accepted 13 August 2002; published 8 October 2002.

[1] Methane ( $\text{CH}_4$ ) emission controls are found to be a powerful lever for reducing both global warming and air pollution via decreases in background tropospheric ozone ( $\text{O}_3$ ). Reducing anthropogenic  $\text{CH}_4$  emissions by 50% nearly halves the incidence of U.S. high- $\text{O}_3$  events and lowers global radiative forcing by  $0.37 \text{ W m}^{-2}$  ( $0.30 \text{ W m}^{-2}$  from  $\text{CH}_4$ ,  $0.07 \text{ W m}^{-2}$  from  $\text{O}_3$ ) in a 3-D model of tropospheric chemistry. A 2030 simulation based upon IPCC A1 emissions projections shows a longer and more intense U.S.  $\text{O}_3$  pollution season despite domestic emission reductions, indicating that intercontinental transport and a rising  $\text{O}_3$  background should be considered when setting air quality goals. **INDEX TERMS:** 0325 Atmospheric Composition and Structure: Evolution of the atmosphere; 0345 Atmospheric Composition and Structure: Pollution—urban and regional (0305); 0368 Atmospheric Composition and Structure: Troposphere—constituent transport and chemistry. **Citation:** Fiore, A. M., D. J. Jacob, B. D. Field, D. G. Streets, S. D. Fernandes, and C. Jang, Linking ozone pollution and climate change: The case for controlling methane, *Geophys. Res. Lett.*, 29(19), 1919, doi:10.1029/2002GL015601, 2002.

### 1. Introduction

[2] There is growing interest in linking air quality and climate change mitigation objectives in the design of emission control strategies. Tropospheric  $\text{O}_3$  deserves particular attention as both the primary constituent of smog [*National Research Council (NRC)*, 1991] and a significant greenhouse gas [*Prather et al.*, 2001]. Ozone is produced in the troposphere by photochemical oxidation of volatile organic compounds (VOC) and carbon monoxide (CO) in the presence of nitrogen oxides ( $\text{NO}_x$ ). While  $\text{O}_3$  production on global and regional scales is sensitive to  $\text{NO}_x$  emissions from fossil fuel combustion [*NRC*, 1991; *Wang and Jacob*, 1998], reducing these emissions may increase greenhouse warming if the positive forcing from increased  $\text{CH}_4$  concentrations offsets the negative forcing from decreased  $\text{O}_3$  concentrations [*Wild et al.*, 2001].

[3] Methane is a known major source of the tropospheric  $\text{O}_3$  background, but is not generally considered a precursor

to regional  $\text{O}_3$  pollution episodes in surface air because of its long lifetime (8–9 years). Recent recognition that intercontinental transport may contribute to these pollution episodes [*Jacob et al.*, 1999; *Yienger et al.*, 2000; *Wild and Akimoto*, 2001; *Fiore et al.*, 2002; *Li et al.*, 2002] raises the profile of  $\text{CH}_4$ . The present-day U.S.  $\text{O}_3$  standard is based upon a 0.08 ppmv (8-hour average), not to be exceeded more than three times per year. If this standard becomes more stringent, as it is in European countries (55–65 ppbv), the relative contribution of the background component to exceedances of the standard will increase. We show that reductions in  $\text{CH}_4$  emissions deserve consideration as a means to meet air quality standards while simultaneously lessening radiative forcing.

### 2. Model Description

[4] We apply GEOS-CHEM (v4.16), a 3-D global model of tropospheric  $\text{O}_3$ - $\text{NO}_x$ -CO-VOC chemistry [*Bey et al.*, 2001], to investigate the response of U.S. pollution episodes and global  $\text{O}_3$  and  $\text{CH}_4$  to (1) 50% reductions in various anthropogenic precursor emissions relative to a 1995 base year and (2) projected 2030 emissions from the IPCC A1 and B1 scenarios [*Prather et al.*, 2001], which project relatively pessimistic and optimistic futures, respectively. All simulations were spun up for 6 months, long enough to remove the effects of initial  $\text{O}_3$  concentrations on the results. Our simulations use assimilated observations of meteorological fields from NASA GEOS-1 with 20 vertical sigma layers and a  $4^\circ \times 5^\circ$  horizontal resolution; comparison with  $2^\circ \times 2.5^\circ$  resolution shows no significant bias [*Fiore et al.*, 2002].

[5] The coarse resolution precludes the model from capturing the local  $\text{O}_3$  maxima that determine compliance with the national  $\text{O}_3$  standard. These maxima, however, typically occur under regionally stagnant conditions that are conducive to the formation of elevated  $\text{O}_3$  levels spanning large spatial scales ( $>600,000 \text{ km}^2$ ) [*Logan*, 1989] resolved by the model. During the summer of 1995, these stagnation episodes occurred more frequently than would be predicted by climatological averages [*McNider et al.*, 1998]. We have previously shown that GEOS-CHEM captures these regional high- $\text{O}_3$  events, as well as the frequency distribution of  $\text{O}_3$  at U.S. sites [*Fiore et al.*, 2002]. We compare here simulated June–August daily afternoon (1–5 p.m. local time) mean  $\text{O}_3$

**Table 1.** Annual Emissions and Growth Factors in GEOS-CHEM<sup>a</sup>

| Species                      | Global    |     |                            |     | United States |     |               |     |
|------------------------------|-----------|-----|----------------------------|-----|---------------|-----|---------------|-----|
|                              | Emissions |     | Growth Factor <sup>b</sup> |     | Emissions     |     | Growth Factor |     |
|                              | 1995      |     | A1 2030                    |     | 1995          |     | A1 2030       |     |
|                              | A         | N   | A                          | N   | A             | N   | A             | N   |
| NO <sub>x</sub>              | 27        | 15  | 1.8                        | 1.0 | 6.6           | 0.6 | 0.8           | 1.0 |
| CO                           | 580       | 630 | 1.2                        | 1.2 | 86            | 17  | 0.6           | 1.1 |
| VOC <sup>c</sup>             | 58        | 450 | 1.6                        | 1.0 | 12            | 33  | 0.7           | 1.0 |
| CH <sub>4</sub> <sup>d</sup> | 340       | 230 | 1.3 <sup>e</sup>           | –   | –             | –   | –             | –   |

<sup>a</sup>A = anthropogenic; N = natural (includes biomass burning). Emissions are in units of Tg N yr<sup>-1</sup> for NO<sub>x</sub>, Tg CO for CO, Tg C for VOC and Tg CH<sub>4</sub> for CH<sub>4</sub>.

<sup>b</sup>Ratio of 2030 to 1995 emissions. Natural emissions remain constant except biomass burning in 2030 A1.

<sup>c</sup>Nonmethane volatile organic compounds; natural emissions include biogenic isoprene (404 Tg C), propene (12 Tg C), acetone (15 Tg C), biomass burning.

<sup>d</sup>The contribution from U.S. emissions is not resolved because a uniform mixing ratio is applied (see text).

<sup>e</sup>Calculated as described in the text.

concentrations with surface measurements at EPA AIRS sites averaged onto the GEOS-CHEM grid in the eastern U.S. (east of 97.5°W where the network is most dense). The correlation coefficient (*r*) between observed and simulated daily afternoon concentrations is 0.68. The percentages of total grid-square afternoons (92 summer afternoons times 27 grid-squares) in excess of 80 ppbv, 70 ppbv, and 60 ppbv, are 5%, 15%, and 36%, respectively, in the observations; the corresponding percentages in the model are 1%, 10%, and 37%, respectively. In this study, we adopt a threshold of 70 ppbv as a metric for polluted conditions since the model provides good statistics for the occurrence of events above this threshold.

[6] The GEOS-CHEM emissions are described in detail by *Bey et al.* [2001] and *Martin et al.* [2002]. We classify biomass burning emissions as natural, following *Fiore et al.* [2002]. The anthropogenic contributions to total global emissions for NO<sub>x</sub>, CO, CH<sub>4</sub> and NMVOC in the base case 1995 simulation (Table 1) are 65%, 50%, 60% and 12%, respectively. The CH<sub>4</sub> concentration for 1995 is fixed at its uniform observed value of 1700 ppbv. This value implies a global emission of 570 Tg CH<sub>4</sub> yr<sup>-1</sup>, computed from mass balance with the simulated global sink (oxidation by OH), plus a 4.9 ppbv yr<sup>-1</sup> tropospheric accumulation. Following *Prather et al.* [2001], we view 60% of CH<sub>4</sub> emissions as anthropogenic. We use the relationship

between CH<sub>4</sub> emissions and concentrations (assuming an OH feedback factor of 1.6) determined by *Prather* [1996] to translate a 50% decrease in anthropogenic CH<sub>4</sub> emissions into a steady-state concentration of 1000 ppbv for the corresponding troposphere.

[7] Emissions for the A1 and B1 2030 scenarios were generated by scaling 1995 emissions by regional growth factors derived from emissions in the IMAGE socioeconomic model [*IMAGE Team*, 2001] for each anthropogenic source and biomass burning. The IMAGE model gives projections consistent with those of the IPCC reference models. Due to space restrictions, we focus here on the A1 scenario. Emissions increase globally (Table 1) from 1995 to 2030, but the distribution shifts. In the developed world (Europe, North America, Japan, etc.), anthropogenic NO<sub>x</sub> emissions decline by 10%, but they increase by 130% in the developing world (South America, Africa, Asia, etc.). U.S. anthropogenic emissions of O<sub>3</sub> precursors decline by 20–40%. IMAGE projects a 43% increase in CH<sub>4</sub> emissions from 1995 to 2030, which we apply to the CH<sub>4</sub> concentration assuming constant OH. In the 2030 A1 simulation, CH<sub>4</sub> actually increases by 31% (as implied by mass balance) because OH concentrations decrease. Thus our CH<sub>4</sub> increase is conservative. The IPCC A1 scenario does not include aircraft NO<sub>x</sub> emissions; we use projections from the Environmental Defense Fund [*Henderson et al.*, 1999] to determine a growth factor of 2.26.

### 3. Impacts on Global Chemistry and Climate

[8] Table 2 summarizes the important results from our simulations. We find that the CH<sub>4</sub> lifetime is longer when NO<sub>x</sub> emissions are decreased and shorter when VOC or CO emissions are decreased, consistent with our understanding of the effect of these emissions on global OH [*Wang and Jacob*, 1998]. The 2030 A1 simulation yields a CH<sub>4</sub> lifetime that is 10% longer than in 1995. The global O<sub>3</sub> production efficiency (OPE), the number of tropospheric O<sub>3</sub> molecules produced per molecule of NO<sub>x</sub> emitted [*Liu et al.*, 1987], increases with decreasing NO<sub>x</sub> emissions and decreases with increasing VOC or CO concentrations (Table 2), again as expected [*Wang and Jacob*, 1998]. The OPE decreases in the A1 simulation, due to the large increase in global fossil fuel NO<sub>x</sub> emissions.

[9] We find that 50% reductions in anthropogenic CH<sub>4</sub> emissions have more influence on the tropospheric O<sub>3</sub>

**Table 2.** Impacts of Perturbations to Anthropogenic Emissions<sup>a</sup>

| Selected Diagnostics                             | Base Case 1995 | 50% CH <sub>4</sub>                                 | 50% NO <sub>x</sub> | 50% VOC | 50% NO <sub>x</sub> & VOC | 50% CO | 50% All | A1 2030 |
|--|----------------|---|---------------------|---------|---------------------------|--------|---------|---------|
| Tropospheric O <sub>3</sub> burden (Tg)          | 321            | 294   | 300                 | 317     | 297                       | 317    | 269     | 394     |
| global CH <sub>4</sub> conc. <sup>b</sup> (ppbv) | 1700           | 1000  | 1867                | 1685    | 1846                      | 1643   | 1040    | 2431    |
| OPE <sup>c</sup>                                 | 33             | 30  | 43                  | 32      | 42                        | 32     | 38      | 27      |
| CH <sub>4</sub> lifetime <sup>d</sup>            | 8.5            | 7.2   | 9.4                 | 8.5     | 9.3                       | 8.3    | 7.5     | 9.3     |
|  |                | U.S. summer afternoon surface O <sub>3</sub> (ppbv) |                     |         |                           |        |         |         |
| Mean   | 51             | 48  | 42                  | 50      | 41                        | 50     | 38      | 55      |
| Background <sup>e</sup>                          | 23             | 21  | 21                  | 23      | 21                        | 23     | 18      | 29      |

<sup>a</sup>Emissions from biomass burning are considered natural [*Fiore et al.*, 2002].

<sup>b</sup>Concentrations are specified for the base case, A1, and 50% CH<sub>4</sub> simulations. For the other simulations, concentrations are derived from the model computed OH concentrations by assuming the same CH<sub>4</sub> source as in the 1995 base case simulation.

<sup>c</sup>Ozone Production Efficiency (OPE) is defined as the ratio of O<sub>3</sub> (actually odd oxygen) production to total NO<sub>x</sub> emissions, following the procedure used by *Wang and Jacob* [1998].

<sup>d</sup>Total atmospheric burden of CH<sub>4</sub> (4760 Tg in GEOS-CHEM) divided by tropospheric loss of CH<sub>4</sub> by reaction with OH.

<sup>e</sup>Background is defined as O<sub>3</sub> produced outside of the North American boundary layer [*Fiore et al.*, 2002] (see text).

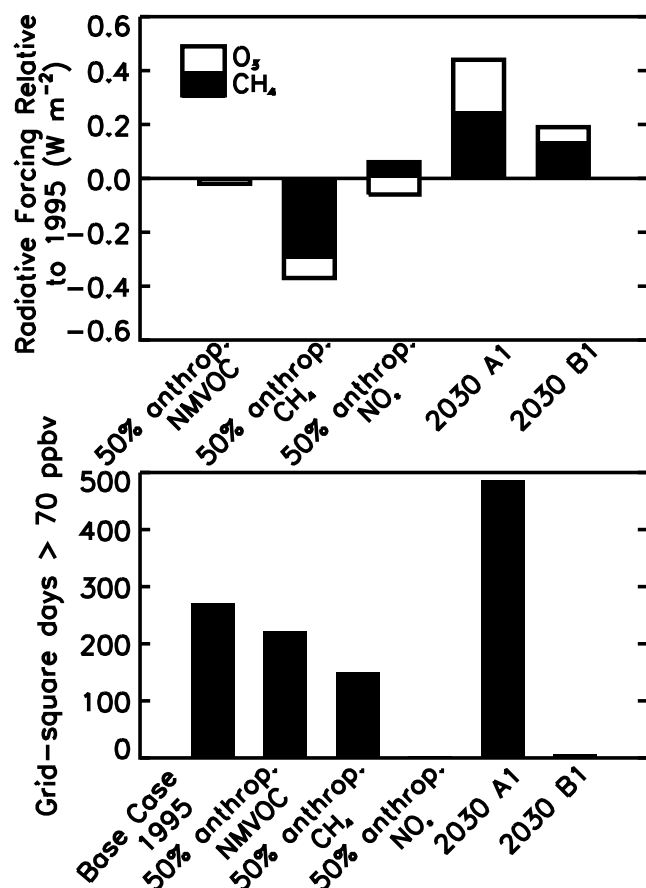


**Figure 1.** Response of radiative forcing and U.S. air quality to (1) 50% global decreases in anthropogenic emissions relative to 1995, (2) IPCC A1 and B1 emissions projections for 2030. (upper panel) Global radiative forcing relative to 1995 as calculated from changes in  $CH_4$  and  $O_3$  concentrations. (lower panel) Number of model grid-square days in the U.S. in summer with mean afternoon (1–5 p.m.) surface  $O_3$  concentrations in excess of 70 ppbv.

burden (Table 2) than 50% reductions in anthropogenic  $NO_x$  emissions. This might appear to be inconsistent with the  $O_3$  source inferred from scaling global  $NO_x$  emissions by the OPEs in Table 2. But, anthropogenic  $NO_x$  emissions have low OPEs due to chemical nonlinearity and titration by  $NO_x$  [Liang *et al.*, 1998; Kasibhatla *et al.*, 1998]. Thus, anthropogenic  $NO_x$  emissions are less effective than natural (in particular from lightning) in contributing to the global  $O_3$  budget, whereas the homogeneity of  $CH_4$  permits anthropogenic and natural  $CH_4$  emissions to be equally effective.

[10] Climatic implications of an atmospheric perturbation can be assessed using the standard concept of radiative forcing [Ramaswamy *et al.*, 2001] which describes the instantaneous global change in the radiative balance of the Earth system resulting from the perturbation. We calculate the change in radiative forcing from  $CH_4$  directly from the global change in concentration [Ramaswamy *et al.*, 2001], while for  $O_3$  we use a relationship of  $0.034 W m^{-2}$  per Dobson Unit change in the mean tropospheric column

[Mickley *et al.*, 1999; Ramaswamy *et al.*, 2001]. Results are shown in the top panel of Figure 1. A 50% reduction in anthropogenic  $CH_4$  emissions yields the largest decrease in radiative forcing ( $-0.37 W m^{-2}$ ;  $-0.30 W m^{-2}$  from  $CH_4$  and  $-0.07 W m^{-2}$  from  $O_3$ ). The radiative effect of 50% reductions in anthropogenic  $NO_x$  emissions is neutral, as the positive forcing due to decreased  $O_3$  is balanced by the negative forcing from increased  $CH_4$  [Fuglestedt *et al.*, 1999]. Both 2030 simulations show positive forcing from 1995 to 2030 (A1:  $0.44 W m^{-2}$ , B1:  $0.19 W m^{-2}$ ).

#### 4. Impacts on U.S. $O_3$ Pollution

[11] We next examine how summertime (June–August) surface air quality over the U.S. responds to the perturbed emissions, focusing on afternoons (1–5 p.m. local time) when  $O_3$  concentrations typically peak. We define background  $O_3$  as that produced outside of the North American boundary layer (surface to 700 hPa). It is diagnosed by applying production and loss rates archived from the full chemical simulation to drive an off-line simulation where  $O_3$  is divided into individual tagged tracers which are produced in different regions of the atmosphere [Fiore *et al.*, 2002]. Table 2 shows mean and background  $O_3$  concentrations simulated on summer afternoons in surface air over the U.S. Summer afternoon  $O_3$  concentrations respond most strongly to the 50% reductions in anthropogenic  $NO_x$  emissions, but reductions in  $CH_4$  emissions also have a large effect. The decreases in  $NO_x$  and  $CH_4$  emissions, however, are equally effective at lowering background  $O_3$  concentrations (2 ppbv in the mean). Decreases in CO or VOC emissions have little impact. For the A1 2030 simulation, mean afternoon surface  $O_3$  increases by 4 ppbv while background concentrations rise by 6 ppbv. Even in the more optimistic B1 scenario, higher global  $CH_4$  emissions contribute to elevating U.S. background  $O_3$  levels by 2 ppbv, partially offsetting air quality gains achieved via domestic emissions controls.

[12] We use a threshold of 70 ppbv as a metric to gauge changes in the frequency of  $O_3$  pollution events in our simulations. Figure 1 (bottom panel) shows the number of U.S. grid-square days in June–August 1995 where simulated afternoon average (1–5 p.m. local time)  $O_3$  levels exceed 70 ppbv. Reducing anthropogenic  $NO_x$  emissions by 50% nearly eliminates the occurrence of grid-square days in excess of 70 ppbv (Figure 1). Because of subgrid variability in  $O_3$ , this result does not mean that local exceedances of 70 ppbv would be as drastically reduced, but it does point to significant improvement in air quality. When anthropogenic  $CH_4$  emissions are reduced by 50%, the incidence of  $O_3$  concentrations in excess of 70 ppbv (Figure 1) declines by 45% (for an 80 ppbv threshold that statistic is 54%).

[13] The U.S. has aggressive emission controls to abate future  $O_3$  pollution. Although fossil fuel emissions in the U.S. for  $NO_x$ , CO, and VOC decline in the IPCC A1 2030 scenario relative to 1995 by 27%, 45%, and 30%, respectively, we find that the number of grid-square summer days over the U.S. with  $O_3 > 70$  ppbv increases relative to 1995. Efforts to improve U.S. air quality are thus thwarted by the rise in global background  $O_3$  levels due to increased emissions outside U.S. borders. These results are consistent with the modeling study of Collins *et al.* [2000] who found

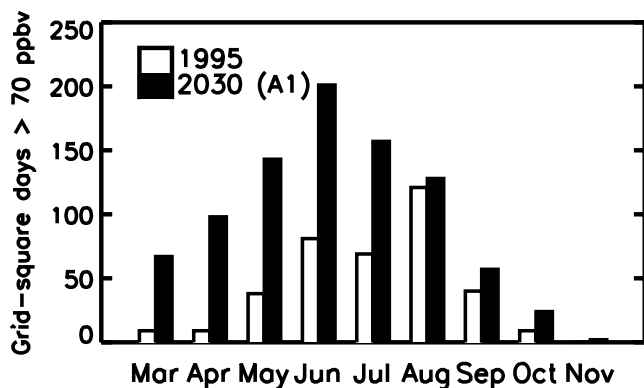


**Figure 2.** Number of U.S. model grid-square days per month with afternoon (1–5 p.m.) O<sub>3</sub> concentrations in surface air above a 70 ppbv threshold for the 1995 base case (white bars) and 2030 A1 (black bars) simulations. The A1 simulation reveals a longer O<sub>3</sub> pollution season. Results are similar for an 80 ppbv O<sub>3</sub> threshold.

that European efforts to improve air quality via domestic emissions reductions may be offset by a rise in emissions from developing nations by 2015. These simulations underscore the need to consider regional air quality in a global context.

[14] Another adverse impact of rising global emissions on U.S. air quality is a longer U.S. O<sub>3</sub> pollution season, as diagnosed by exceedances of a 70 ppbv threshold. Intercontinental transport makes a larger contribution to U.S. O<sub>3</sub> pollution in spring and fall than in summer because of the longer O<sub>3</sub> lifetime [Jacob *et al.*, 1999]. Figure 2 shows the larger numbers of exceedances of the 70 ppbv threshold in March through November in the A1 2030 simulation; results are similar for an 80 ppbv threshold. Relatively small changes in mean U.S. O<sub>3</sub> concentrations resulting from a higher global O<sub>3</sub> background are thus sufficient to extend the U.S. O<sub>3</sub> pollution season into April–May.

## 5. Conclusions

[15] Our global 3-D model analysis shows that reducing CH<sub>4</sub> emissions enables a simultaneous pursuit of O<sub>3</sub> air quality and climate change mitigation objectives. Whereas reductions in NO<sub>x</sub> emissions achieve localized decreases in surface O<sub>3</sub> concentrations, reductions in CH<sub>4</sub> emissions lower the global O<sub>3</sub> background and improve surface air quality everywhere. Simulation of a 2030 (IPCC A1) scenario where anthropogenic U.S. emissions of O<sub>3</sub> precursors decrease but global emissions (including CH<sub>4</sub>) increase indicates a greater incidence of O<sub>3</sub> pollution episodes and a longer U.S. O<sub>3</sub> season, stressing the need for a global perspective in the design of future regional pollution control strategies.

[16] **Acknowledgments.** The authors would like to thank Loretta Mickley and Mat Evans for helpful conversations, and to acknowledge the support of the U.S. EPA Office of Air Quality and Planning Standards, the National Science Foundation, and the Atmospheric Chemistry Modeling and Analysis Program of NASA.

## References

- Bey, I., et al., Global modeling of tropospheric chemistry with assimilated meteorology: Model description and evaluation, *J. Geophys. Res.*, *106*, 23,073–23,096, 2001.
- Collins, W. J., et al., The European regional ozone distribution and its links with the global scale for the years 1992 and 2015, *Atmos. Environ.*, *34*, 255–267, 2000.
- Fiore, A. M., et al., Background ozone over the United States in summer: Origin, trend, and contribution to pollution episodes, *J. Geophys. Res.*, *107*(D15), 10.1029/2001JD000982, 2002.
- Fuglestedt, J. S., et al., Climatic forcing of nitrogen oxides through changes in tropospheric ozone and methane: Global model studies, *Atmos. Environ.*, *33*, 961–967, 1999.
- Henderson, S. C., and U. K. Wickrama, Aircraft Emissions: Current Inventories and Future Scenarios, in *Aviation and the Global Atmosphere*, edited by J. E. Penner et al., Cambridge Univ. Press, Cambridge, 1999.
- IMAGE Team, *The Image 2.2 implementation of the SRES scenarios*, [RIVM CD-ROM publication 481508018], National Institute for Public Health and the Environment, Bilthoven, The Netherlands, July 2001.
- Jacob, D. J., J. A. Logan, and P. P. Murti, Effect of Rising Asian Emissions on Surface Ozone in the United States, *Geophys. Res. Lett.*, *26*, 2175–2178, 1999.
- Kasibhatla, P., et al., Relationships between regional ozone pollution and emissions of nitrogen oxides in the eastern United States, *J. Geophys. Res.*, *103*, 22,663–22,669, 1998.
- Liang, J., et al., Seasonal variations of reactive nitrogen species and ozone over the United States, and export fluxes to the global atmosphere, *J. Geophys. Res.*, *103*, 13,435–13,450, 1998.
- Li, Q., et al., Transatlantic Transport of Pollution and its Effects on Surface Ozone in Europe and North America, *J. Geophys. Res.*, 10.1029/2001JD001422, 2002.
- Liu, S. C., et al., Ozone Production in the Rural Troposphere and the Implications for Regional and Global Ozone Distributions, *J. Geophys. Res.*, *92*, 4191–4207, 1987.
- Logan, J. A., Ozone in Rural Areas of the United States, *J. Geophys. Res.*, *94*, 8511–8532, 1989.
- Martin, R. V., et al., Interpretation of TOMS observations of tropical tropospheric ozone with a global model and in situ observations, *J. Geophys. Res.*, 10.1029/2001JD001480, 2002.
- McNider, R. T., et al., Meteorological conditions during the 1995 Southern Oxidants Study Nashville/Middle Tennessee Field Intensive, *J. Geophys. Res.*, *103*, 22,225–22,243, 1998.
- Mickley, L. J., et al., Radiative forcing from tropospheric ozone calculated with a unified chemistry-climate model, *J. Geophys. Res.*, *104*, 30,153–30,172, 1999.
- National Research Council (NRC), *Rethinking the Ozone Problem in Urban and Regional Air Pollution*, Nat. Acad. Press, Washington, D.C., 1991.
- Prather, M. J., Time scales in atmospheric chemistry: Theory, GWPs for CH<sub>4</sub> and CO, and runaway growth, *Geophys. Res. Lett.*, *23*, 2597–2600, 1996.
- Prather, M. J., et al., Atmospheric Chemistry and Greenhouse Gases, in *Climate Change 2001*, edited by J. T. Houghton et al., pp. 239–287, Cambridge Univ. Press, Cambridge, 2001.
- Ramaswamy, V., et al., Radiative Forcing of Climate Change, in *Climate Change 2001*, edited by J. T. Houghton et al., pp. 349–416, Cambridge Univ. Press, Cambridge, 2001.
- Wang, Y., and D. J. Jacob, Anthropogenic forcing on tropospheric ozone and OH since preindustrial times, *J. Geophys. Res.*, *103*, 31,123–31,135, 1998.
- Wild, O., M. J. Prather, and H. Akimoto, Indirect long-term global radiative cooling from NO<sub>x</sub> Emissions, *Geophys. Res. Lett.*, *28*, 1719–1722, 2001.
- Wild, O., and H. Akimoto, Intercontinental transport of ozone and its precursors in a three-dimensional global CTM, *J. Geophys. Res.*, *106*, 27,729–27,744, 2001.
- Yienger, J. J., et al., The episodic nature of air pollution transport from Asia to North America, *J. Geophys. Res.*, *105*, 26,931–26,945, 2000.

A. M. Fiore, D. J. Jacob, and B. D. Field, Department of Earth and Planetary Sciences and Division of Engineering and Applied Sciences, Harvard University, Cambridge, MA 02138, USA.

D. G. Streets and S. D. Fernandes, Argonne National Laboratory, DIS/900, 9700 South Cass Avenue, Argonne, IL 60439, USA.

C. Jang, USEPA/OAQPS MC: D243-01, 109 T.W. Alexander Drive, RTP, NC 27711, USA.